

# StyleDiff: Attribute Comparison Between Unlabeled Datasets in Latent Disentangled Space

Keisuke Kawano\*      Takuro Kutsuna      Ryoko Tokuhisa  
 Akihiro Nakamura      Yasushi Esaki

Toyota Central R&D Labs., Inc.

\*kawano@mosk.tytlabs.co.jp

## Abstract

One major challenge in machine learning applications is coping with mismatches between the datasets used in the development and those obtained in real-world applications. These mismatches may lead to inaccurate predictions and errors, resulting in poor product quality and unreliable systems. In this study, we propose StyleDiff to inform developers of the differences between the two datasets for the steady development of machine learning systems. Using disentangled image spaces obtained from recently proposed generative models, StyleDiff compares the two datasets by focusing on attributes in the images and provides an easy-to-understand analysis of the differences between the datasets. The proposed StyleDiff performs in  $O(dN \log N)$ , where  $N$  is the size of the datasets and  $d$  is the number of attributes, enabling the application to large datasets. We demonstrate that StyleDiff accurately detects differences between datasets and presents them in an understandable format using, for example, driving scenes datasets.

## 1 Introduction

One of the major challenges in machine learning applications is handling the mismatches between the dataset used in the development and those obtained in real-world applications. In this study, we refer to the dataset obtained from the real-world application as *real dataset* and that used during development as *development dataset*. Note that the development dataset is used to train and test the models, design the model architectures, and create specification.

Informing the developers of the distinction between the two datasets can be aided by detailing their associated attributes. In datasets, some attributes are explicitly labeled as recognition targets, while most attributes are not. For example, for an object detection system in autonomous vehicles that detects cars and pedestrians, each training image is labeled to indicate whether these targets are included in the image, while other attributes,

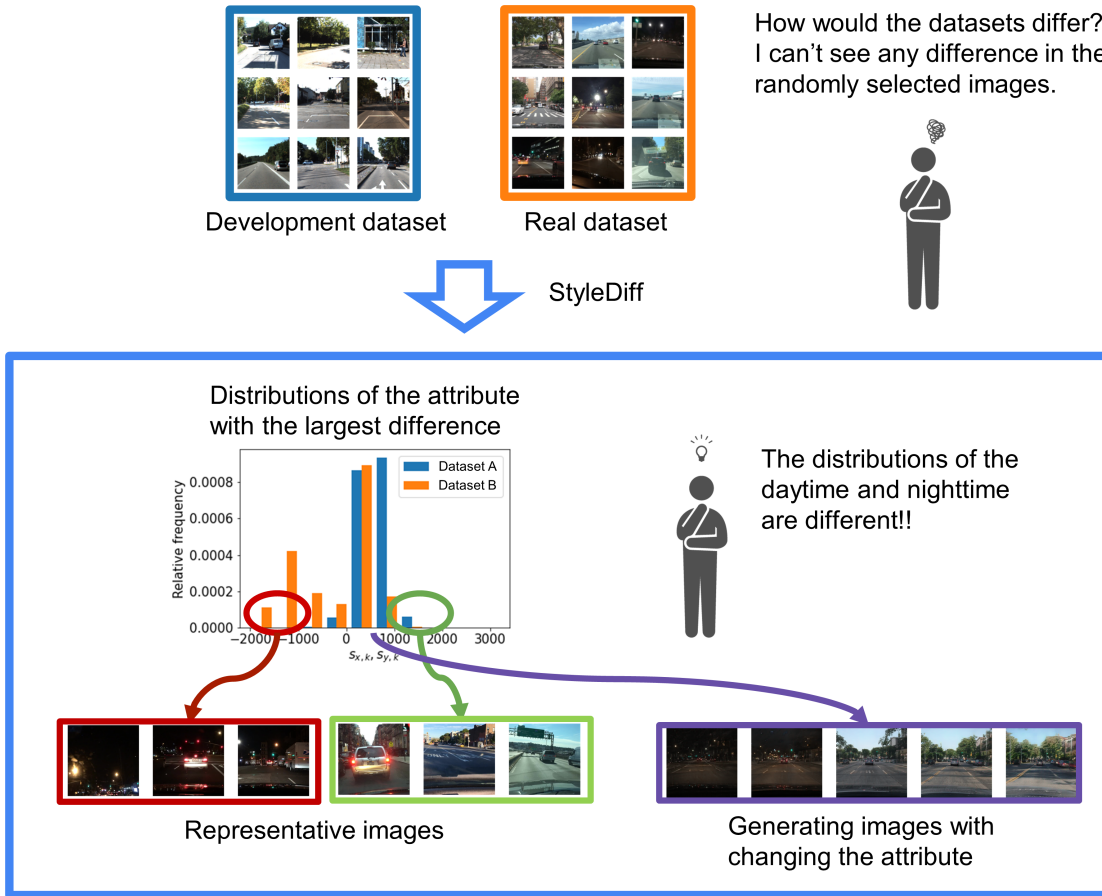


Figure 1: Concept of StyleDiff. StyleDiff compares the distributions of attributes extracted from the two input datasets. StyleDiff presents information about the attributes that differ in their distributions using the histograms, representative images, and images generated by changing the attribute.

such as road conditions, the time of day, and congestion level, may not be explicitly labeled. Moreover, the real dataset are typically unlabeled. The absence of certain attributes in the development dataset that are present in the real dataset can lead to inadequate training, testing, and poor accuracy, resulting in low product quality and unreliable machine learning systems. We aim to provide developers with attributes that have different distributions in the two datasets to avoid problems caused by the mismatch, without manually defining these attributes and labeling the attributes to each image.

One approach used to present the difference between the two datasets is to select the representative images from the datasets [20, 9, 27]. This approach allows us to specify images that represent the difference between the real and development datasets without labeled information. However, the approach still has two challenges.

- The difference between the two datasets is only visualized as selected images, making

it difficult to infer which attributes are differently distributed in these datasets. Various attributes, such as road conditions, weather, and position of surrounding vehicles, coexist in an image. Furthermore, even when there are differences between datasets with multiple attributes, existing methods can only provide a single image set with a mixture of images representing the multiple attributes. This makes it more difficult for the developers to understand which attributes differ in distributions.

- Because existing methods are formulated as discrete optimization problems, some are computationally difficult to apply to large datasets containing tens of thousands of images. For example, the computational complexity of PWC [20] and the coresets approach (k-center greedy)<sup>1</sup> [9, 27] are  $O(N^2)$ , where  $N$  is the number of images in the datasets.

In this study, we propose StyleDiff, a method for comparing attribute distributions in two datasets. We demonstrate the concept of StyleDiff in Figure 1. The proposed StyleDiff compares the distributions of attributes extracted from the real and development datasets, and then presents information regarding the attributes that differ in their distributions using, for example, histograms of the distributions, representative images, and generated images. Even when there are differences between multiple attribute distributions, StyleDiff visualizes these attributes individually by selecting the attributes and providing images for each of the selected attributes. One difficulty with implementing StyleDiff is that the two datasets do not contain explicit information about the attributes. Therefore, to realize StyleDiff, it is necessary to extract the attributes from the dataset, and then compare the distributions of the attributes. To extract the various attribute information from each image, we propose using the disentangled space obtained from the generative models [18, 19, 29]. The disentangled space facilitates comparison between datasets straightforwardly.

Our contributions are summarized as follows.

- We propose StyleDiff that visualizes the attributes with different distributions in the two unlabeled datasets.
- We show that the computational complexity of the StyleDiff is  $O(dN \log N)$ , where  $N$  is the number of images and  $d$  is the number of extracted attributes when a pretrained encoder is available, allowing StyleDiff to be applied to large datasets.
- Experimentally, we demonstrate that StyleDiff outperforms existing methods in extracting images correspond to the differences between the datasets. Furthermore, using real-world datasets, we demonstrate that StyleDiff can present the attributes individually, even when there are differences among multiple attributes.

The rest of this paper is organized as follows. In Section 2, we describe our proposed StyleDiff. Section 3 presents a literal review of related work. Subsequently, in Section 4, we show some numerical experiments to demonstrate StyleDiff. Finally, in Section 5, we present our conclusion.

---

<sup>1</sup>Note that for the dataset covering problems [20], the distances between  $N$  candidate points in one dataset and  $N$  centers in the other dataset are required.

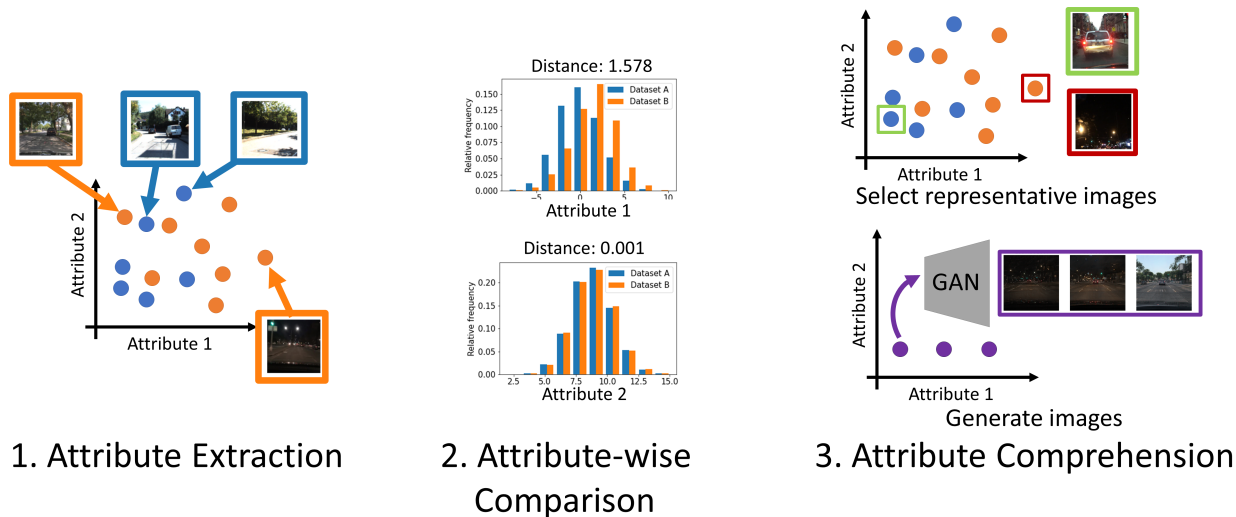


Figure 2: Overview of StyleDiff. StyleDiff first extracts attribute distributions from the two unlabeled datasets. The distributions are then compared to identify the attributes that have large differences. Finally, to show the users the identified attributes, StyleDiff presents attributes by selecting some images at the specific locations in the distributions and/or generating images by changing the attribute.

## 2 StyleDiff

StyleDiff identifies attributes that differ in their distribution by comparing two datasets. StyleDiff leverages the embedding space of images, where each dimension ideally has a one-to-one correspondence with a single attribute; that is each dimension of the embedding space controls a single attribute (disentanglement) and each attribute is controlled by a single dimension (completeness). We call the embedding space *attribute space* and the embedding vectors *attribute vectors*. For the attribute space, we employ the latent space of the recently developed GAN [19, 3], which is known for its high disentanglement and completeness [29]. Using the attribute space, StyleDiff extracts the attributes that differ in their distributions and presents them in an easy-to-understand form. As illustrated in Figure 2, StyleDiff comprises the following three steps.

1. Attribute Extraction: transform each image in the two datasets into an attribute vector.
2. Attribute-Wise Comparison: calculate the distances between the distributions for each attribute using the attribute vectors and select attributes based on the distances.
3. Attribute Comprehension: visualize the selected attributes by selecting images from the datasets according to the distributions of the attributes or by generating images using a generator.

In the following, we describe each of them individually.

**Notations** Vectors and matrices are denoted in bold style (e.g.,  $\mathbf{x}$ ,  $\mathbf{A}$ ).  $\mathbf{1}_N \in \mathbb{R}^N$  represents an  $N$ -dimensional vector with all elements being ones.  $\mathbb{R}_+$  is a set of real positive numbers. The  $L_p$  norm is denoted as  $\|\cdot\|_p$ . For a natural number  $N$ ,  $\llbracket N \rrbracket$  means  $\{1, \dots, N\}$ .  $\delta_a$  is the Dirac delta at  $a \in \mathbb{R}$ .

## 2.1 Attribute Extraction

The proposed method converts all images  $\mathbf{x}^{(i)}, \mathbf{y}^{(j)} \in \mathbb{R}^{H \times W \times 3}$  in two datasets  $A = \{\mathbf{x}^{(i)} \mid i \in \llbracket N_x \rrbracket\}$  and  $B = \{\mathbf{y}^{(j)} \mid j \in \llbracket N_y \rrbracket\}$  into attribute vectors  $\mathbf{s}_x^{(i)}, \mathbf{s}_y^{(j)} \in \mathbb{R}^d$ , where  $d$  denotes the number of dimensions for the attribute vectors. As attribute vectors, we can use style vectors [29] obtained from StyleGAN2 [19] and Restyle encoder [3] trained on the same domain as the two datasets.

Style vectors, intermediate latent vectors of StyleGAN2, are renowned for their disentangled and complete latent space called StyleSpace [19]. Let  $\mathbf{z} \in \mathbb{R}^{d_{\text{in}}}$  be a latent vector of StyleGAN2, where  $d_{\text{in}}$  is the dimension of the vector, and StyleGAN2 first transforms it into the style vector using a feedforward neural network  $f : \mathbb{R}^{d_{\text{in}}} \mapsto \mathbb{R}^d$  as  $f(\mathbf{z})$ . Subsequently, StyleGAN2 generates an image from the style vector as  $G(f(\mathbf{z}))$ , where  $G : \mathbb{R}^d \mapsto \mathbb{R}^{H \times W \times 3}$  is the generator function. To obtain the style vectors corresponding to the images in the datasets, we employ the Restyle encoder [3]  $h : \mathbb{R}^{H \times W \times 3} \mapsto \mathbb{R}^{d_{\text{in}}}$ , which predicts the latent vectors  $\mathbf{z}$  corresponding to the input image  $\mathbf{x}$ .

We denote the function to convert images into attribute vectors as  $\phi : \mathbb{R}^{H \times W \times 3} \mapsto \mathbb{R}^d$ . By applying  $\phi$  to images  $\mathbf{x}^{(i)}$  and  $\mathbf{y}^{(j)}$ , the following two sets of attribute vectors can be obtained.

$$\mathcal{S}_x = \{\mathbf{s}_x^{(i)} \mid i \in \llbracket N_x \rrbracket\}, \quad \mathcal{S}_y = \{\mathbf{s}_y^{(j)} \mid j \in \llbracket N_y \rrbracket\}, \quad (1)$$

where  $\mathbf{s}_x^{(i)} = \phi(\mathbf{x}^{(i)})$  and  $\mathbf{s}_y^{(j)} = \phi(\mathbf{y}^{(j)})$ . With the composite function of the Restyle encoder and the feedforward network of StyleGAN2  $\phi = f \circ h : \mathbb{R}^{H \times W \times 3} \mapsto \mathbb{R}^d$ , we can obtain the style vectors corresponding to the images in the datasets.

## 2.2 Attribute-Wise Comparison

StyleDiff calculates the distance between the two sets of attribute vectors for each dimension of the attribute space. Because each dimension of the attribute space is expected to correspond to an attribute in the images, this process is equivalent to calculating the distance between the two distributions for each attribute. For the sets of attribute vectors  $\mathcal{S}_x$  and  $\mathcal{S}_y$ , we extract the  $c$ -th dimensional values and define the following two empirical distributions  $X_c$  and  $Y_c$  for each dimension.

$$X_c = \frac{1}{N_x} \sum_{i=1}^{N_x} \delta_{s_{x,c}^{(i)}} \quad Y_c = \frac{1}{N_y} \sum_{j=1}^{N_y} \delta_{s_{y,c}^{(j)}}, \quad (2)$$

where  $s_{x,c}^{(i)}, s_{y,c}^{(j)} \in \mathbb{R}$  are  $c$ -th values of  $\mathbf{s}_x^{(i)}$  and  $\mathbf{s}_y^{(j)}$ , respectively.

StyleDiff employs the Wasserstein distance  $\mathcal{W}(X_c, Y_c)$  [25] to evaluate the dissimilarities between the empirical distributions. The Wasserstein distance requires no additional hyper-parameters, such as kernels, and can be obtained rapidly, as described in Section 2.5. The Wasserstein distance between the empirical distributions is defined as follows:

$$\mathcal{W}(X_c, Y_c) = \left( \min_{\mathbf{P} \in U(\mathbf{m}_x, \mathbf{m}_y)} \sum_{i=1}^{N_x} \sum_{j=1}^{N_y} P_{ij} D_{c,ij} \right)^{\frac{1}{2}}, \quad (3)$$

$$U(\mathbf{m}_x, \mathbf{m}_y) = \{\mathbf{P} \in [0, 1]^{N_x \times N_y} \mid \mathbf{P}^\top \mathbf{1}_{N_x} = \mathbf{m}_y, \mathbf{P} \mathbf{1}_{N_y} = \mathbf{m}_x\}, \quad (4)$$

where  $\mathbf{P}$  is the matrix representing the transport plan, and its  $(i, j)$ -element  $P_{ij}$  represents the mass transported from  $\mathbf{x}^{(i)}$  to  $\mathbf{y}^{(j)}$ .  $\mathbf{m}_x = [\frac{1}{N_x}, \dots, \frac{1}{N_x}]^\top \in \mathbb{R}_+^{N_x}$  and  $\mathbf{m}_y = [\frac{1}{N_y}, \dots, \frac{1}{N_y}]^\top \in \mathbb{R}_+^{N_y}$  are the masses for the images.  $U(\mathbf{m}_x, \mathbf{m}_y)$  corresponds the mass conservation constraints.  $D_{c,ij}$  is the cost of transporting the mass from  $s_{x,c}^{(i)}$  to  $s_{y,c}^{(j)}$ . For example, the following squared Euclidean distance is often used:

$$D_{c,ij} = \|\mathbf{s}_{x,c}^{(i)} - \mathbf{s}_{y,c}^{(j)}\|_2^2 \quad (5)$$

StyleDiff calculates the distances  $\mathcal{W}(X_c, Y_c)$  for all  $c \in \llbracket d \rrbracket$ , and selects  $K$  dimensions with the largest distances. We denote the selected dimensions sorted by the distances as  $\mathbf{c}^* = [c_1^*, \dots, c_K^*]$ .

We propose normalizing distances between attribute vectors based on their scales, as the scales have a greater impact on the distance than the attribute distributions' differences when the scales differ significantly (see Section 4.2). We can normalize the cost of transportation (Eq. (5)) as  $D_{ij} = \frac{1}{\sigma_c^2} |s_{x,c}^{(i)} - s_{y,c}^{(j)}|^2$ , where  $\sigma_c$  is the standard deviation of  $\{s_{x,c}^{(i)} \mid i \in \llbracket N_x \rrbracket\} \cup \{s_{y,c}^{(j)} \mid j \in \llbracket N_y \rrbracket\}$ . This normalization aligns the scale of the attribute vectors on all dimensions, eliminating the influence of the scales.

## 2.3 Attribute Comprehension

The selected dimensions  $\mathbf{c}^*$  are expected to correspond to attributes in the images. To understand the attributes corresponding to each selected dimension  $c_l^* \in \mathbf{c}^*$ , we propose two methods. One is selecting representative images from the two datasets based on the  $c_l^*$ -th values of the attribute vectors (i.e.,  $s_{x,c_l^*}^{(i)}$  and  $s_{y,c_l^*}^{(j)}$ ), for example, images corresponding to the endpoints with maximum or minimum values, or images corresponding to the region where the difference between the two distributions is significant. The other is generating an image sequence, in which only the corresponding attribute is varied, by changing the  $c_l^*$ -th value of an attribute vector using the StyleGAN2 [19]. An image sequence in which only one attribute is varied clearly informs the user which attribute corresponds to the  $c_l^*$ -th dimension of the attribute space. The proposed StyleDiff can be used for the dataset covering problems [20] by selecting representative images, such as images at the endpoint of the dimension with the largest distance.

## 2.4 Attribute Vector Modification

We experimentally found that an attribute may correspond to multiple dimensions of StyleSpace depending on the learned domain. When an attribute corresponds to multiple dimensions, i.e., low completeness, a problem in visualizing the attributes may occur, as described in Section 4.3. We propose mitigating this problem by applying principal component analysis (PCA) to the style vectors, as in [16]. By applying PCA, highly correlated dimensions in the style vectors are combined into one. Note that PCA does not only increase the completeness but also decreases the disentanglement, i.e., several correlated attributes may be combined into a single dimension.

## 2.5 Computational Complexity

Let  $N = \max\{N_x, N_y\}$  be the number of images in the datasets and  $K$  be the number of dimensions to select. Given a function  $\phi$  that converts each image into an attribute vector, the computational complexity of converting images into attribute vectors is  $O(N_x + N_y)$ . The dimension-wise Wasserstein distances can be calculated by  $O(dN \log N)$  [25] since  $s_{x,c}^{(i)}$  and  $s_{y,c}^{(j)}$  are scalar values. In addition, visualization of the selected attributes requires  $O(K)$  for image generation, and  $O(N)$  for image selection, (e.g., images with minimum and maximum values). Therefore, the total computational complexity of the proposed method is  $O(dN \log N)$ , enabling StyleDiff to be applied to large datasets.

StyleDiff requires the function  $\phi$  such as Restyle encoder [3] trained in the same domain as the two target datasets. It is challenging to accurately estimate the amount of computation needed for training GAN encoders; however, we emphasize that they have been effectively trained on datasets of over 10,000 images in practice.

## 3 Related Work

**Dataset covering** The problem of selecting the representative images from datasets to represent the difference between the datasets is formulated as a dataset covering problem [20]. Methods for addressing the dataset covering the problem include PWC, anomaly detection, and active learning methods. PWC visualizes which patterns in one dataset are missing in another dataset by selecting data points to minimize the partial Wasserstein divergence [25] between the real dataset and union of the development dataset and selected data points. Anomaly detection methods [11, 26, 21, 7] can be considered a method of detecting the difference between datasets in terms of detecting data in one dataset that is missing in another. Active learning methods [17, 13, 27, 28] can also be used to extract data in one dataset that cannot be correctly predicted by a model trained on another dataset. Unlike these methods, StyleDiff aims to compare the two datasets by their attribute distributions, and to visualize the difference between them. The proposed method enables us to select and generate images corresponding to attributes and to compare the histograms of the attributes. This rich information is useful for developers to investigate missing patterns in the development dataset.

**Geometric dataset distance** The optimal transport distances, which are typically defined between a set of vectors or scalar values, have recently attracted considerable attention in machine learning community [25, 14, 8]. The optimal transport theory can be used to define distances between unordered sets of arbitrary length, such as datasets [20, 5]. The optimization problem of the Wasserstein distance is a linear programming problem and can be solved, for example, exactly using the interior-point method or approximately by Sinkhorn iterations [14, 10, 25]. In the worst-case scenario, their computational complexity is  $O(N^3)$  and  $O(TN^2)$ , respectively, where  $N$  is the number of data points and  $T$  is the number of iterations. As a special case, it is also known that the Wasserstein distance can be computed in  $O(N \log N)$  when the dimension of vectors  $d$  is equal to 1 [25].

In addition to solving the dataset covering problem [20], the optimal transport distances between datasets can be used, for example, to evaluate the difficulty of transfer learning [5] and to find correspondences between data in cross-lingual datasets [6]. In StyleDiff, we compare the two datasets by finding the optimal transport distances in attribute-wise sliced space, rather than in multidimensional embedding spaces. This allows for an attribute-wise comparison of the two datasets and reduces the computational complexity to  $O(N \log N)$  per dimension.

**StyleSpace** StyleSpace, which is a disentangled space for images [29, 16], has been used for several tasks [3, 24, 4, 22, 12]. Image manipulation is a popular application of the StyleSpace [3, 24, 4]. By changing some elements of the style vector corresponding to an input image and decoding it, we can obtain an image in which only some attributes are edited. Lang et al., employed StyleSpace to illustrate a trained classifier [22] as another example of an application. StyleDiff also uses the disentangled StyleSpace for the attribute-wise comparison of two datasets, however, our objective (i.e., comparing two datasets) is distinct from these methods.

## 4 Experiment

In this section, we demonstrate how StyleDiff determines and visualizes the difference in attributes between the given two datasets through numerical experiments. First, we apply StyleDiff to two artificially generated datasets with different distributions of an attribute to demonstrate the functionality of the proposed method. A quantitative evaluation of the ability to identify attributes with varying distributions was conducted by applying the proposed and existing methods to artificially generated datasets. Finally, we illustrate StyleDiff in a realistic scenario by comparing two driving scene datasets. The implementations of StyleGAN2 [19] and Restyle [3] used in the following experiments are the publicly available ones [1, 2], respectively. The training of StyleGAN2 was performed on an NVIDIA Tesla A100, and all other computations were performed on an NVIDIA RTX TITAN. All hyperparameters used during training are default values of the public implementations [1, 2].

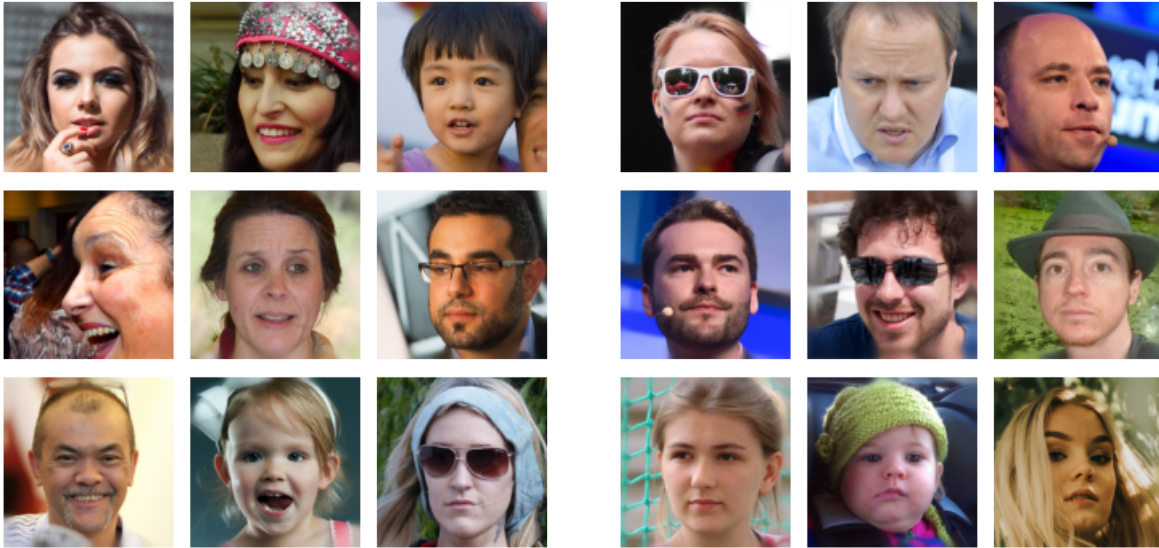
(a) Dataset *A*(b) Dataset *B*

Figure 3: Examples randomly drawn from two generated datasets (FFHQ [18])

#### 4.1 Demonstration: Artificially Generated Datasets

In this subsection, we demonstrate how the attributes are extracted and visualized by the proposed method using two datasets that are artificially generated to ensure that their distributions in an attribute are different. The two datasets are generated by randomly sampling 5,000 images for each from the FFHQ dataset [18], which is a dataset of human face images. To generate the two datasets, we use the publicly available attributes <sup>2</sup> of the FFHQ dataset. There are 34 attributes estimated from the images, including categorical values (e.g., beard) and continuous values (e.g., age).

We generate two datasets with different distributions of smiling, which is one of the attributes. One dataset *A* contains 75% of smiling people and 25% of non-smiling people, while another dataset *B* contains 25% of smiling people and 75% of non-smiling people. In this experiment, we convert the degrees of smiling (i.e., continuous values from 0 to 1) into a binary label with a threshold of 0.5. Figure 3 illustrates examples that are randomly drawn from the two generated datasets. As shown in Figure 3, the images contain various attributes (e.g., face orientation, hairstyle, and brightness), rendering it challenging to distinguish the two datasets merely by examining the examples.

Given the two generated datasets, we demonstrate how the datasets are compared and how the attribute (i.e., smiling) is detected and visualized by StyleDiff. In the experiment, the attribute vectors are style vectors obtained from the publicly available pretrained Restyle encoder [3, 1] and StyleGAN2 [19, 2], which are trained on the FFHQ dataset. The dimension of the attribute space ( $d$ ) is 6,048.

After transforming each image in the two datasets into an attribute vector, StyleDiff

<sup>2</sup><https://github.com/DCGM/ffhq-features-dataset>

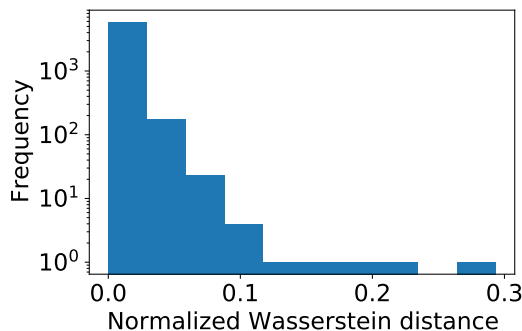
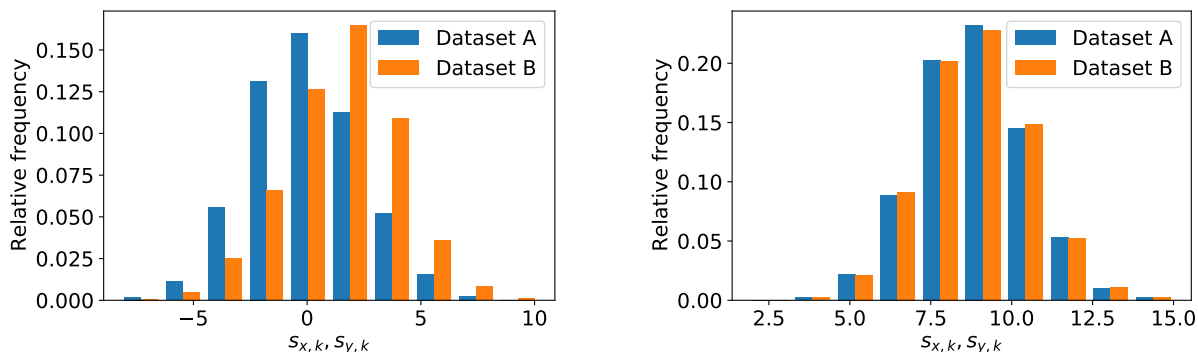


Figure 4: Histogram of dimension-wise distances between two datasets



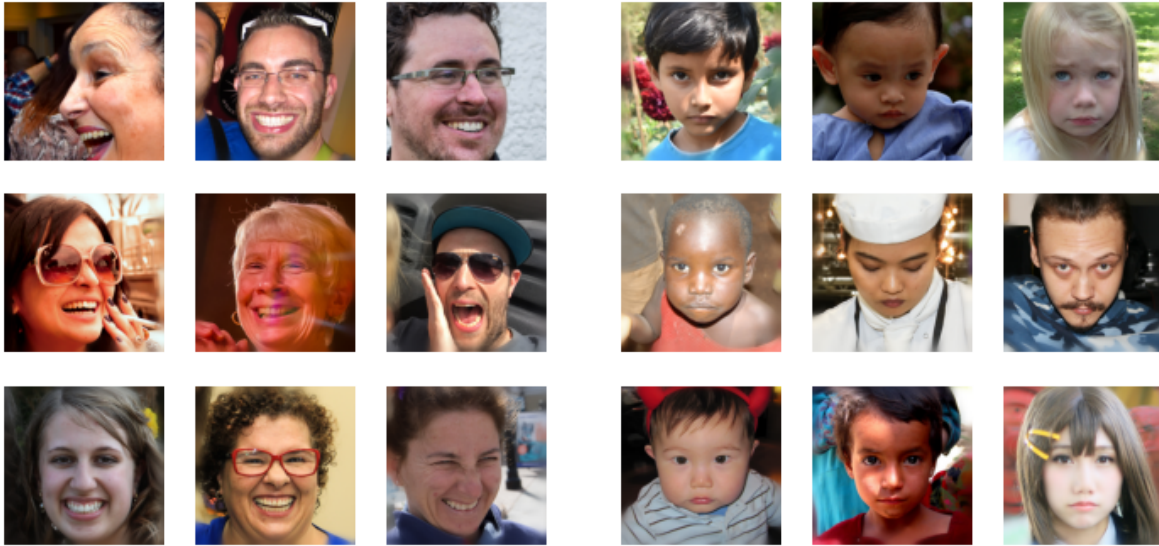
(a) Distribution of the attribute vectors on the dimension with the largest distance

(b) Distribution of the attribute vectors on the dimension with the smallest distance

Figure 5: Distribution of the attribute vectors

determines the distances between the set of the attribute vectors  $\mathcal{S}_x, \mathcal{S}_y$  for each dimension of the attribute space. The histogram of the dimension-wise distances between two datasets is shown in Figure 4. As illustrated in Figure 4, only two dimensions have values above 0.2 while the remaining 6046 dimensions have values close to zero. This implies that the attribute vectors have high completeness; that is, an attribute is controlled by a few dimensions of the attribute space. We also illustrate the distribution of the attribute vectors on the dimension with the largest distance (Wasserstein distance: 0.293) and on the dimension with the smallest distance (Wasserstein distance: 0.000) in Figure 5. As shown in Figure 5, the difference between the two distributions can be quantified using the Wasserstein distance, which can be rapidly computed for a set of scalar values.

StyleDiff allows us to select dimensions by distance and visualize the corresponding attributes. Here, for example, we select the dimension with the largest distance and visualize the corresponding attribute. The images that exist at the endpoints of the selected dimension are shown in Figure 6. As shown in Figures 6 (a) and (b), the images in Figure 6 (a) are all smiling images, while those in Figure 6 (b) are all non-smiling images. The rest of the



(a) Images with low values on the selected dimension

(b) Images with high values on the selected dimension

Figure 6: Results of StyleDiff: Attribute comprehension via representative images. The images correspond to the endpoints of the dimension with the largest distance (Fig. 5 (a)).

attributes vary in Figures 6 (a) and (b). This indicates that the selected dimension corresponds to the smile attribute. We can assess the bias of the attribute (Smiling) in the two datasets by comparing their distributions in Figure 5 (a).

We then demonstrate the visualization of the attribute by generating an image sequence. Figure 7 (a) is a generated image obtained by the trained StyleGAN2 [19] with a random input vector. By gradually changing the values in the selected dimension of the corresponding attribute vector, Figure 7 (b) can be obtained. In Figure 7 (b), only one attribute, i.e., the degree of smiling, varies gradually, while all the other attributes (e.g., background, face orientation, and hairstyle) are invariant. The image sequence reveals that the selected dimension corresponds to the degree of smiling. As shown in this demonstration, StyleDiff allows us to identify attributes with different distributions between two datasets that could not be discovered by only looking at the examples in Figure 3.

## 4.2 Quantitative Evaluation

We quantitatively compare StyleDiff and existing methods (PWC [20], LOF [11], and coresets (k-center greedy) [27]) in terms of their ability to detect differences between two unlabeled datasets. Following [20], we quantify the ability to select the images from the development dataset corresponding to the attribute that is less included in the development dataset than in the real dataset.

For the evaluation, we similarly generate two datasets to the method in Section 4.1. A subset of 500 images sampled from the FFHQ dataset [19] was used for each of the datasets.



(a) Generated image with the random latent vector



(b) Generated image sequence by gradually changing the values of the selected dimension of the corresponding attribute vector

Figure 7: Results of StyleDiff: Attribute comprehension via generated images

The development dataset and the real dataset are sampled so that the proportions of the binary labels  $l \in \{0, 1\}$  (e.g., smiling and non-smiling) are  $p : (1 - p)$  and  $(1 - p) : p$ , where  $p \in [0, 0.5]$ , respectively. For the binary labels, continuously-valued attributes are scaled from 0 to 1 and then converted to binary labels with a threshold of 0.5. For categorical values (e.g., NoGlasses, ReadingGlasses, and Sunglasses for the glasses attribute), we select the most common one for the binary label  $l = 0$ , and the others for  $l = 1$ . If both continuous and categorical values are available for an attribute, the continuous value is used for the label. If there are fewer than 500 images for a binary label, the corresponding attributes are not evaluated. We evaluate a total of 26 attributes.

We apply the proposed StyleDiff and existing methods to the two datasets and then quantitatively evaluate their ability to detect the attributes that are less included in the development dataset. As a metric, we use  $r_p^{(l)}$ , which is the percentage of images with the label  $l$  in the 10 images selected from the real dataset. We compare the averages of  $r_p^{(l)}$ , i.e.,  $\frac{1}{2} \sum_{l \in \{0, 1\}} \frac{1}{11} \sum_{p \in \{0, 0.05, \dots, 0.5\}} r_p^{(l)}$ .

For StyleDiff, all images in the two datasets are converted into the style vectors using the trained StyleGAN2 [19, 1] and the trained Restyle encoder [3, 2], and used as the attribute vectors as in Section 4.1. To apply StyleDiff to the dataset covering the problem, we select the dimension with the largest distance and then present the images in the real dataset at the endpoint. To determine which of the two endpoints to select, we compare the means of the two distributions on the dimension and select one that is closer to the mean of the real dataset than that of the development dataset. In addition to the proposed method, we evaluate existing methods, PWC (PW-sensitivity-ent) [20], LOF [11], and coresets(k-center greedy) [27], using the same datasets. According to [20], we use pretrained ResNet50 [23] for the embedding vectors required by existing methods. As an ablation, we also evaluate the proposed StyleDiff, where the distances are not scaled according to the scales of the attribute vectors (SD w/o normalize). The expectation of the evaluation score is 0.75.

The average of the scores for 10 trials with different random seeds for the sampling is pre-

Table 1: Quantitative evaluation results. SD denotes StyleDiff.

Attribute Name	SD	SD w/o normalize	PWC[20]	LOF [11]	k-center[9, 27]
Smile	<b>0.882</b>	0.813	0.774	0.753	0.755
Age	<b>0.911</b>	0.871	0.805	0.752	0.744
Blur-value	<b>0.770</b>	0.752	0.768	0.748	0.750
Exposure-value	<b>0.855</b>	0.836	0.771	0.753	0.740
Gender	0.917	<b>0.921</b>	0.810	0.741	0.756
EyeMakeup	<b>0.885</b>	0.883	0.807	0.753	0.759
LipMakeup	<b>0.875</b>	0.843	0.805	0.759	0.767
Glasses	0.920	<b>0.929</b>	0.797	0.748	0.745
Moustache	0.915	<b>0.920</b>	0.815	0.760	0.770
Beard	<b>0.911</b>	0.910	0.802	0.730	0.742
Sideburns	<b>0.930</b>	0.917	0.795	0.730	0.737
Noise-value	<b>0.807</b>	0.778	0.766	0.750	0.759
ForeheadOccluded	<b>0.921</b>	0.898	0.837	0.744	0.754
Hair-bald	<b>0.910</b>	0.879	0.798	0.740	0.745
Hair-invisible	<b>0.937</b>	0.894	0.836	0.744	0.765
HairColor-brown	<b>0.759</b>	0.750	0.742	0.755	0.741
HairColor-blond	0.752	<b>0.753</b>	0.738	0.734	0.718
HairColor-black	<b>0.786</b>	0.748	0.769	0.753	0.767
HairColor-red	<b>0.810</b>	0.779	0.747	0.744	0.737
HairColor-gray	0.810	<b>0.830</b>	0.785	0.735	0.742
HeadPose-pitch	<b>0.880</b>	0.835	0.750	0.751	0.739
HeadPose-roll	<b>0.813</b>	0.810	0.751	0.749	0.759
HeadPose-yaw	<b>0.927</b>	0.924	0.749	0.755	0.746
Emotion-happiness	<b>0.882</b>	0.813	0.773	0.753	0.755
Emotion-neutral	<b>0.884</b>	0.814	0.756	0.748	0.742
Emotion-surprise	<b>0.872</b>	0.865	0.786	0.755	0.762

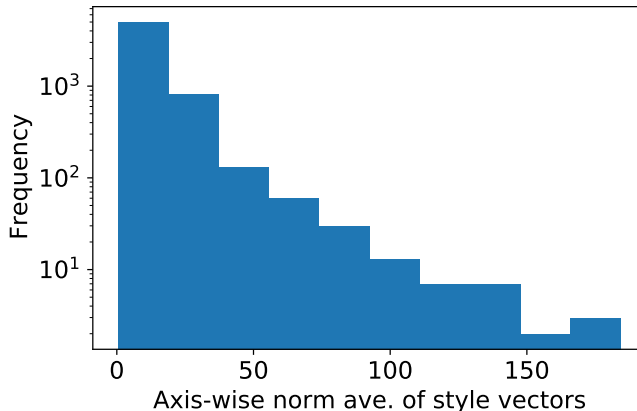


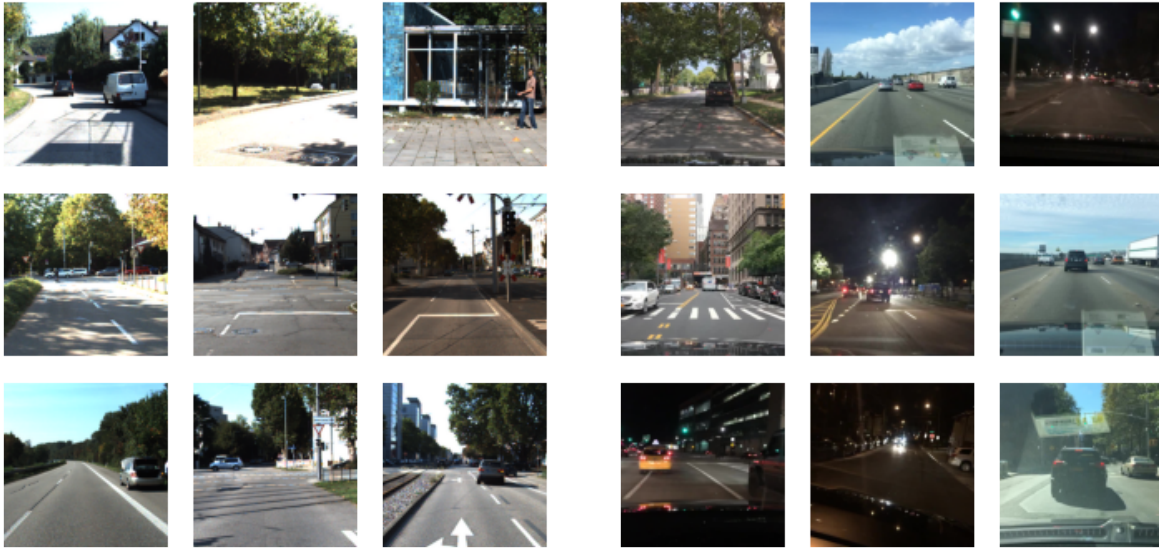
Figure 8: Average norms of the attribute vectors for each dimension

sented in Table 1. Evidently, StyleDiff outperformed the existing methods for all attributes. This indicates that StyleDiff can extract the less included attributes with higher accuracy than the existing methods, including PWC [20]. The ablation study shows that SD with normalization (SD) outperformed SD without normalization (SD w/o normalization) in 21 of the 26 attributes, indicating that scaling improves the performance in finding the target attributes. Figure 8 presents the histogram of the average norms for each dimension of the 10,000 randomly sampled attribute vectors. Figure 8 indicates that the norms vary widely among the dimensions, with a few dimensions above 100 and most around 10. Normalizing the distances removes the effect of the norms and improves the performance of the proposed method.

### 4.3 Comparing Two Driving Scene Datasets

Finally, following to [20], we demonstrate how StyleDiff extracts and visualizes the differences between the two datasets in a realistic situation by applying StyleDiff to widely-used driving scene datasets, KITTI (Object Detection Evaluation 2012) [15] and BDD100k [30]. Both of the datasets contain images captured by vehicle-mounted cameras and are used to train and evaluate object detection models. Figure 9 illustrates images randomly sampled from each dataset. One of the major differences between the datasets is that KITTI contains only daytime images, while BDD100k contains both daytime and nighttime images. In this experiment, we test whether the attribute that differs in the distributions (i.e., time) is correctly extracted by the proposed StyleDiff. We also show the other attributes extracted by the proposed method. The two datasets are compared using all images in the test sets of BDD100k and KITTI. The number of images is 20,000 and 7518, respectively.

To convert the images into the attribute vectors, we trained StyleGAN2 [19] and Restyle encoder [3] using all the images in the training splits of the BDD100k [30] and KITTI [15] datasets. As described below, the style vectors obtained from the trained models were not suitable for the attribute vectors because multiple dimensions in the vectors correspond to



(a) KITTI dataset [15]

(b) BDD100k dataset [30]

Figure 9: Images randomly drawn from KITTI and BDD100k datasets

the same attributes. In this experiment, we apply PCA to the style vectors and use the transformed vectors as the attribute vectors. The number of principal components is set so that the total contribution is 0.99999. In addition to the proposed method, we apply the existing methods, PWC (PW-sensitivity-ent) [20], LOF [11], and coresets(k-center greedy) [27] to the two datasets. All hyperparameters follow to [20]. For PWC [20], we sampled 500 data from each of the two datasets and used them as the input due to GPU memory constraints. We emphasize that StyleDiff can be applied to datasets with over 10,000 images without any sampling processes.

In the following, we first analyze the top-3 dimensions with large distances obtained by StyleDiff, and then present the results of existing methods. Finally, as a limitation of the proposed method, we demonstrate the results of StyleDiff without PCA for the attribute vectors.

**Visualizing the dimension with the largest distance** The distributions of the two datasets on the dimension with the largest distance are presented in Figure 10 (a). We also show the image sequence generated by varying the value of the selected dimension in Figure 10 (b), where the maximum and minimum values for the generation are the mean value  $\pm$  the standard deviation for the union of the two distributions. Figure 10 (b), where the images vary between daytime and nighttime as the values on the dimension vary, indicates that the dimension corresponds to the difference between daytime and nighttime. Figure 10 (a) also shows that the region around -1500 of this dimension contains only BDD100k images. To visualize the region, we randomly select five BDD100k images with values around -1500 and present them in Figure 10 (c). We also show the images of BDD100k and KITTI with values around 1000 in Figures 10 (d) and (e), where KITTI images are more common than

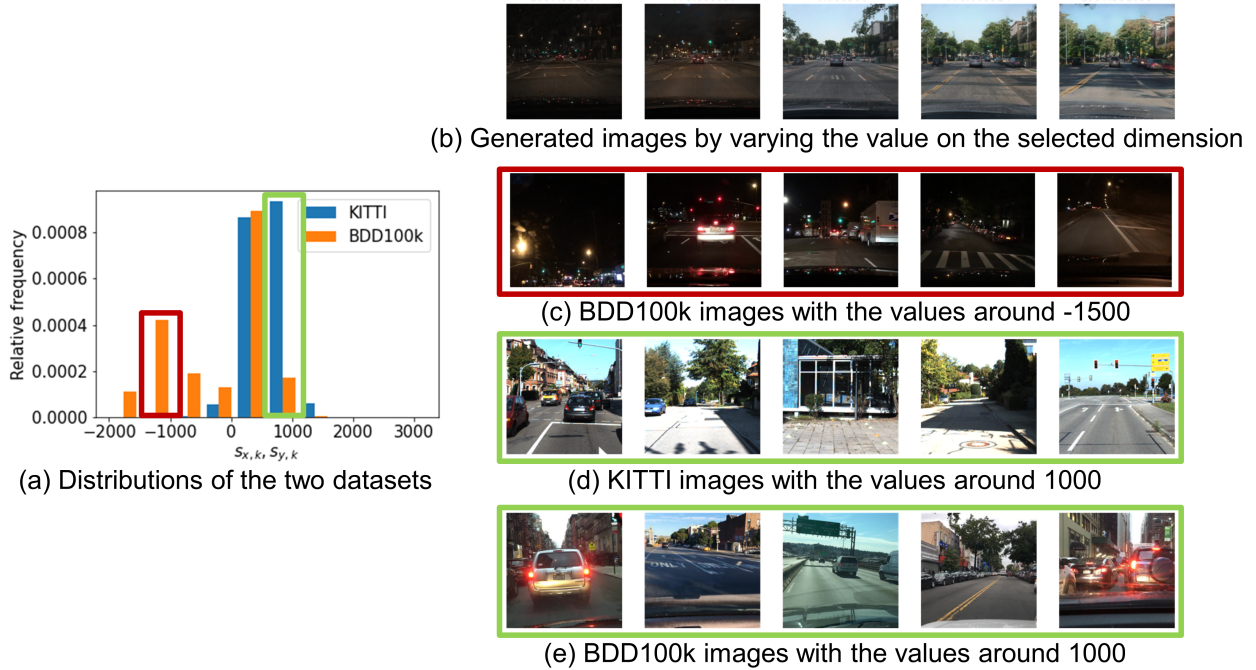


Figure 10: Results of StyleDiff: The dimension with the largest distance ( $c_1^*$ )

BDD100k images. Figures 10 (c), (d), and (e) indicate that the region from -1800 to -500 corresponds to nighttime while the region around 1000 corresponds to daytime. Clearly, StyleDiff can extract the major differences between the BDD100k and KITT datasets (i.e., daytime and nighttime) by comparing their attribute vectors.

**Visualizing the dimension with the second-largest distance** We then visualize the attribute corresponding to the dimension with the second-largest distance. The histogram of the two distributions on this dimension and a sequence of images are presented in Figures 11 (a) and (b), respectively. The generated images in Figure 11 (b) indicate that the dimension corresponds to the density of the background area. The histogram also shows that the region around 2000 contains only KITT images. Most of the images corresponding to this region are shown in Figure 11 (c), illustrating the same building. For the comparison, we also show some images corresponding to the region around -1000 in Figures 11 (d) and (e). Figures 11 (d) and (e) illustrate the open scenes with no buildings in front. From these analyses, we found that BDD100k and KITT differ in their distributions of the background because the KITT dataset contains numerous images captured from the vehicle stopped in front of the building. The proposed StyleDiff can extract attributes differ from the first attribute (daytime and nighttime), although it is impossible to separately visualize multiple attributes using existing methods that only provide a set of images.

**Visualizing the dimension with the third-largest distance** Figure 12 (a) illustrates the distributions of the two datasets on the dimension with the third-largest distance. We also

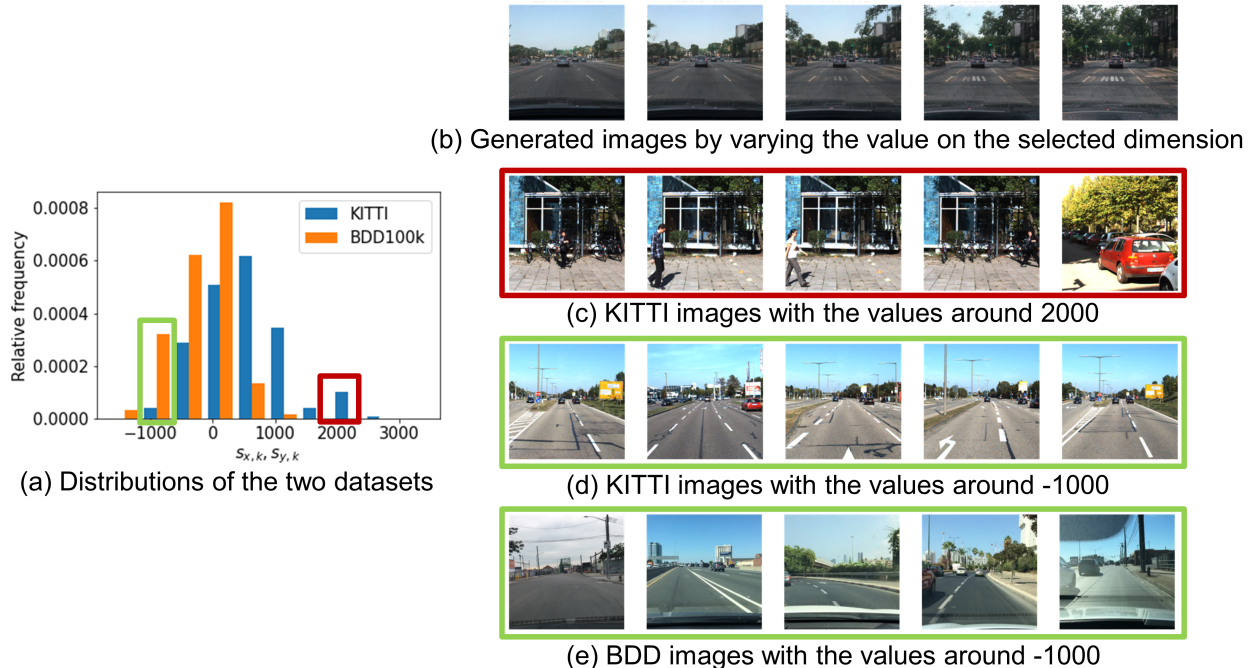


Figure 11: Results of StyleDiff: The dimension with the second-largest distance ( $c_2^*$ )

demonstrate the generated image sequence corresponding to the dimension in Figure 12 (b). From the generated images in Figure 12 (b), the lights in the image, such as traffic lights and tail lights, become more intense as the value of the dimension increases. Figure 12 (a) also indicates that the region above 2000 on the dimension contains one KITTI image and 73 BDD100k images. The images of BDD100k with values around 2000 on the dimension are presented in Figure 12 (c). For comparison, the images of KITTI and BDD100k with values around -700 are shown in Figures 12 (d) and (e). These figures indicate that the third dimension also corresponds to the attribute representing daytime and nighttime, similar to the first dimension. However, unlike the first dimension, which corresponds to the night scenes without lights, the third dimension corresponds to night scenes illuminated by artificial lights (e.g., traffic and tail lights). The proposed StyleDiff allows us to visualize similar attributes separately if they are represented on different dimensions in the attribute vectors. As discussed in this subsection, StyleDiff allows attribute-wise comparisons between the given two datasets. We can analyze the differences between the datasets through the histograms, images in the datasets, and generated images. These detailed attribute-wise analyses can steadily improve and develop reliable machine learning systems.

**Results of existing methods** In Figures 13, 14, and 15, we demonstrate the results of existing methods, PWC [20], LOF [11], and coresets (k-center greedy) [27], on the two datasets, respectively. Because Figure 13 contains several night scenes, users can infer that the KITTI dataset (i.e., the development dataset) has fewer night scenes than the BDD100k

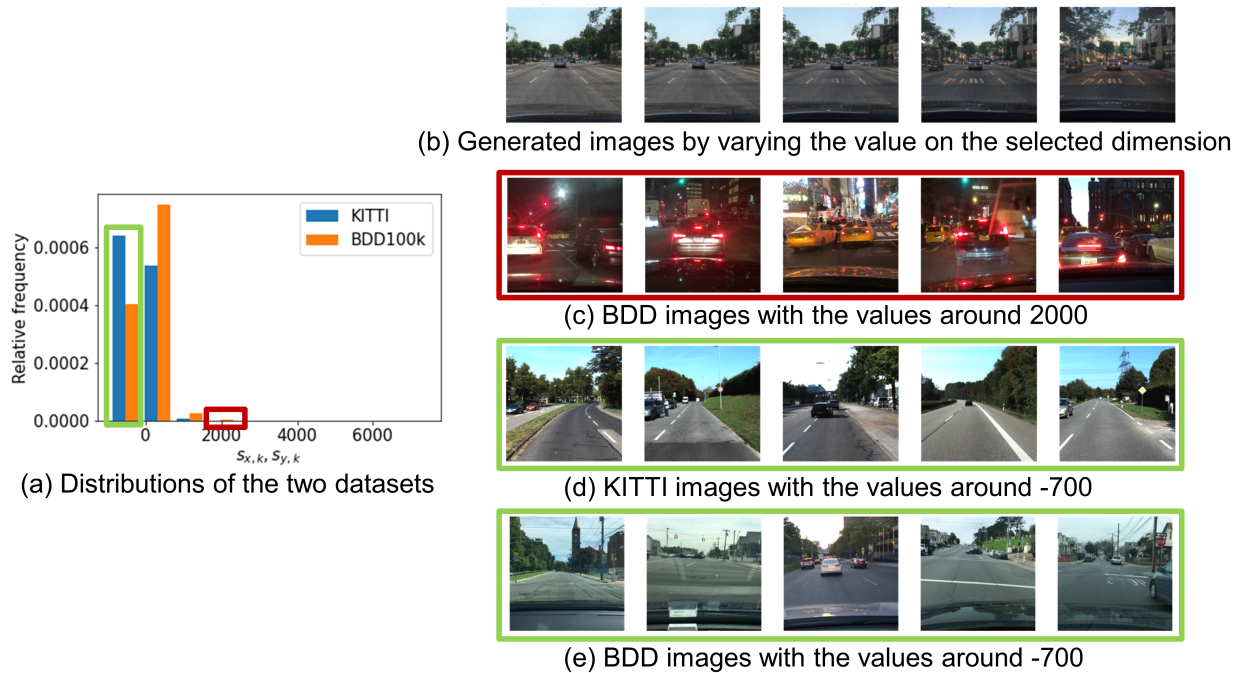


Figure 12: Results of StyleDiff: The dimension with the third-largest distance ( $c_3^*$ )

dataset (i.e., the real dataset). However, it is impossible to investigate how the attribute (i.e., daytime and nighttime) is distributed in the two datasets. Furthermore, it is not even possible to infer if the distributions for the other attributes are different. From the results of the LOF and coresnet, it is difficult to understand the most significant difference (daytime and nighttime) between the two datasets. We also emphasize that StyleDiff allows us to analyze histograms of attribute distributions, obtain images corresponding to specific regions in the histogram, and generate image sequences corresponding to the attributes, although the information regarding attributes obtained by existing methods is only a set of images.

**Failure example: StyleDiff without PCA for driving scene datasets** Because the performance of StyleDiff is influenced by the quality of the attribute space, it is difficult to extract attributes if the disentanglement and completeness of the space are low. The results of StyleDiff with a poor quality attribute space, StyleSpace trained on the driving scene datasets, are presented in Figure 16, where the dimensions corresponding to the top-3 largest distances are visualized. As shown in Figure 16, the endpoints of all the top-3 dimensions correspond to illuminated night scenes and daytime images, indicating that the single attribute corresponds to the multiple dimensions (i.e., low completeness). Here, the generated images did not change even if the values of the selected dimension were changed so that the corresponding attribute could not be visualized by the generated images. This is because multiple dimensions must be changed simultaneously to manipulate the attribute in the image, and changing the value of only one dimension cannot significantly affect the generated images. Note that, on the contrary, if the disentanglement of the attribute space is



Figure 13: Images selected by PWC [20]



Figure 14: Images selected by LOF [11]



Figure 15: Images selected by coreset (k-center greedy) [9, 27]

low, changing the value of a single dimension may change multiple attributes simultaneously, making it difficult to infer the corresponding attributes.

## 5 Conclusion

In this study, we proposed StyleDiff, which compares two image datasets and visualizes the distributions of the attributes. StyleDiff visualizes the attributes by selecting images in the datasets and generating image sequences. Even when there are differences in multiple attribute distributions, the proposed method can provide information about the attributes, separately. The computational complexity of the proposed method is  $O(dN \log N)$ , and it can be applied to datasets with over 10,000 images. Experimentally, we demonstrated that the difference between the two image datasets could be discovered and visualized by the proposed StyleDiff. Furthermore, we demonstrated that StyleDiff outperformed existing methods [20, 11, 9, 27] in detecting the difference between datasets by the quantitative evaluation. StyleDiff’s limitation is the need for attribute vectors, leading to degraded performance when low-quality attribute vectors are employed. By investing the differences between the two datasets via StyleDiff, developers of machine learning systems can understand which attributes are less considered during development. This allows the developers to plan for additional testing and data collection, and to design attribute-specific subroutines for the system, resulting in improved performance and reliable machine learning systems.

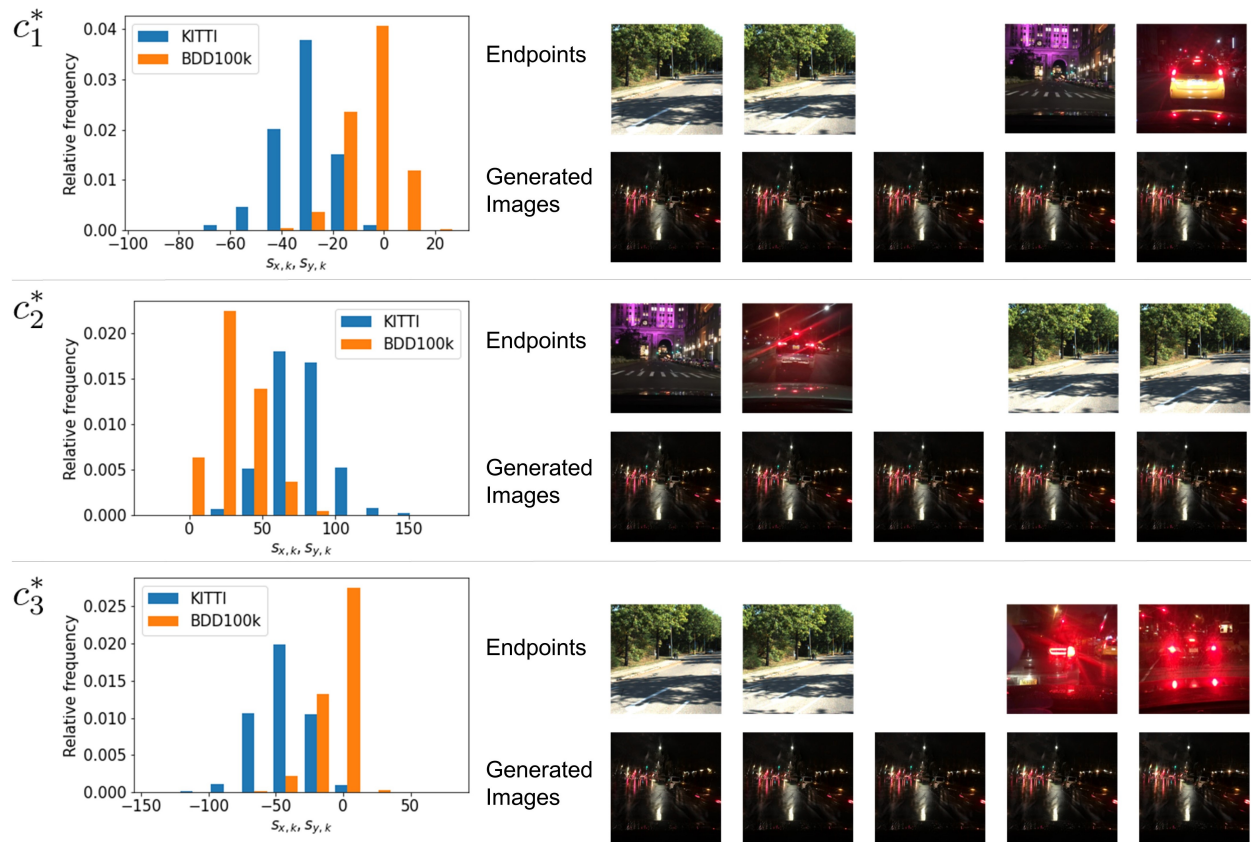


Figure 16: Failure example: comparison results of BDD100k and KITTI when the style vectors are used directly as the attribute vectors

## References

- [1] Alias-Free Generative Adversarial Networks (StyleGAN3) Official PyTorch implementation of the NeurIPS 2021 paper. <https://github.com/NVlabs/stylegan3>, 2021. Accessed: 2022-11-7.
- [2] ReStyle: A Residual-Based StyleGAN Encoder via Iterative Refinement (ICCV 2021). <https://github.com/yuval-alaluf/restyle-encoder>, 2021. Accessed: 2022-12-7.
- [3] Yuval Alaluf, Or Patashnik, and Daniel Cohen-Or. Restyle: A residual-based stylegan encoder via iterative refinement. In *Proceedings of the IEEE/CVF International Conference on Computer Vision*, pages 6711–6720, 2021.
- [4] Yuval Alaluf, Or Patashnik, Zongze Wu, Asif Zamir, Eli Shechtman, Dani Lischinski, and Daniel Cohen-Or. Third time’s the charm? image and video editing with stylegan3, 2022.
- [5] David Alvarez-Melis and Nicolo Fusi. Geometric dataset distances via optimal transport. In H. Larochelle, M. Ranzato, R. Hadsell, M. F. Balcan, and H. Lin, editors, *Advances in Neural Information Processing Systems 33*, volume 33, pages 21428–21439. Curran Associates, Inc., 2020.
- [6] David Alvarez-Melis and Tommi S Jaakkola. Gromov-wasserstein alignment of word embedding spaces. *arXiv preprint arXiv:1809.00013*, 2018.
- [7] Jinwon An and Sungzoon Cho. Variational autoencoder based anomaly detection using reconstruction probability. *Special Lecture on IE*, 2(1):1–18, 2015.
- [8] Martin Arjovsky, Soumith Chintala, and Léon Bottou. Wasserstein generative adversarial networks. In Doina Precup and Yee Whye Teh, editors, *Proceedings of the 34th International Conference on Machine Learning*, volume 70 of *Proceedings of Machine Learning Research*, pages 214–223. PMLR, 06–11 Aug 2017.
- [9] Olivier Bachem, Mario Lucic, and Andreas Krause. Practical coresets constructions for machine learning. *arXiv preprint arXiv:1703.06476*, 2017.
- [10] Jean-David Benamou, Guillaume Carlier, Marco Cuturi, Luca Nenna, and Gabriel Peyré. Iterative bregman projections for regularized transportation problems. *SIAM Journal on Scientific Computing*, 37(2):A1111–A1138, 2015.
- [11] Markus M Breunig, Hans-Peter Kriegel, Raymond T Ng, and Jörg Sander. Lof: identifying density-based local outliers. In *Proceedings of the 2000 ACM SIGMOD International Conference on Management of Data*, pages 93–104, 2000.
- [12] Min Jin Chong, Wen-Sheng Chu, Abhishek Kumar, and David Forsyth. Retrieve in style: Unsupervised facial feature transfer and retrieval. In *Proceedings of the IEEE/CVF International Conference on Computer Vision*, pages 3887–3896, 2021.

- [13] Luiz FS Coletta, Moacir Ponti, Eduardo R Hruschka, Ayan Acharya, and Joydeep Ghosh. Combining clustering and active learning for the detection and learning of new image classes. *Neurocomputing*, 358:150–165, 2019.
- [14] Marco Cuturi. Sinkhorn distances: Lightspeed computation of optimal transport. In *Advances in Neural Information Processing Systems 26*, pages 2292–2300, 2013.
- [15] Andreas Geiger, Philip Lenz, Christoph Stiller, and Raquel Urtasun. Vision meets robotics: The kitti dataset. *International Journal of Robotics Research*, 2013.
- [16] Erik Härkönen, Aaron Hertzmann, Jaakko Lehtinen, and Sylvain Paris. Ganspace: Discovering interpretable gan controls. *Advances in Neural Information Processing Systems*, 33:9841–9850, 2020.
- [17] Alex Holub, Pietro Perona, and Michael C Burl. Entropy-based active learning for object recognition. In *2008 IEEE Computer Society Conference on Computer Vision and Pattern Recognition Workshops*, pages 1–8. IEEE, 2008.
- [18] Tero Karras, Samuli Laine, and Timo Aila. A style-based generator architecture for generative adversarial networks. In *Proceedings of the IEEE/CVF conference on computer vision and pattern recognition*, pages 4401–4410, 2019.
- [19] Tero Karras, Samuli Laine, Miika Aittala, Janne Hellsten, Jaakko Lehtinen, and Timo Aila. Analyzing and improving the image quality of stylegan. In *Proceedings of the IEEE/CVF conference on computer vision and pattern recognition*, pages 8110–8119, 2020.
- [20] Keisuke Kawano, Satoshi Koide, and Keisuke Otaki. Partial wasserstein covering. In *Proceedings of the AAAI Conference on Artificial Intelligence*, volume 36(7), pages 7115–7123, 2022.
- [21] Ki Hyun Kim, Sangwoo Shim, Yongsub Lim, Jongseob Jeon, Jeongwoo Choi, Byungchan Kim, and Andre S Yoon. Rapp: Novelty detection with reconstruction along projection pathway. In *International Conference on Learning Representations*, 2019.
- [22] Oran Lang, Yossi Gandelsman, Michal Yarom, Yoav Wald, Gal Elidan, Avinatan Hassidim, William T Freeman, Phillip Isola, Amir Globerson, Michal Irani, et al. Explaining in style: Training a gan to explain a classifier in stylespace. In *Proceedings of the IEEE/CVF International Conference on Computer Vision*, pages 693–702, 2021.
- [23] Sébastien Marcel and Yann Rodriguez. Torchvision the machine-vision package of torch. In *Proceedings of the 18th ACM International Conference on Multimedia*, pages 1485–1488, 2010.
- [24] Or Patashnik, Zongze Wu, Eli Shechtman, Daniel Cohen-Or, and Dani Lischinski. Styleclip: Text-driven manipulation of stylegan imagery. In *Proceedings of the IEEE/CVF International Conference on Computer Vision*, pages 2085–2094, 2021.

- [25] Gabriel Peyré, Marco Cuturi, et al. Computational optimal transport: With applications to data science. *Foundations and Trends® in Machine Learning*, 11(5-6):355–607, 2019.
- [26] Bernhard Schölkopf, Robert C Williamson, Alexander J Smola, John Shawe-Taylor, John C Platt, et al. Support vector method for novelty detection. In *Advances in Neural Information Processing Systems 12*, volume 12, pages 582–588. Citeseer, 1999.
- [27] Ozan Sener and Silvio Savarese. Active learning for convolutional neural networks: A core-set approach. In *ICLR (Poster)*. OpenReview.net, 2018.
- [28] Changjian Shui, Fan Zhou, Christian Gagné, and Boyu Wang. Deep active learning: Unified and principled method for query and training. In *International Conference on Artificial Intelligence and Statistics*, pages 1308–1318. PMLR, 2020.
- [29] Zongze Wu, Dani Lischinski, and Eli Shechtman. Stylespace analysis: Disentangled controls for stylegan image generation. In *Proceedings of the IEEE/CVF Conference on Computer Vision and Pattern Recognition*, pages 12863–12872, 2021.
- [30] Fisher Yu, Haofeng Chen, Xin Wang, Wenqi Xian, Yingying Chen, Fangchen Liu, Vashisht Madhavan, and Trevor Darrell. Bdd100k: A diverse driving dataset for heterogeneous multitask learning. In *Proceedings of the IEEE/CVF conference on computer vision and pattern recognition*, pages 2636–2645, 2020.